Polyhedron 52 (2013) 115–121

Contents lists available at SciVerse ScienceDirect

Polyhedron

journal homepage: www.elsevier.com/locate/poly

Structure–property trends in cyanido-bridged tetranuclear Fe^{III}/Ni^{II} single-molecule magnets

Yuan-Zhu Zhang [a], Uma Prasad Mallik [a], Rodolphe Clérac [c,d,*], Nigam P. Rath [a,b], Stephen M. Holmes [a,b,*]

[a] Department of Chemistry and Biochemistry, University of Missouri-St. Louis, St. Louis, MO 63121, USA
[b] Center for Nanoscience, University of Missouri-St. Louis, St. Louis, MO 63121, USA
[c] CNRS, UPR 8641, Centre de Recherche Paul Pascal (CRPP), Equipe "Matériaux Moléculaires Magnétiques", 115 avenue du Dr. Albert Schweitzer, 33600 Pessac, France
[d] Université de Bordeaux, UPR 8641, 33600 Pessac, France

ARTICLE INFO

Article history:
Available online 8 November 2012

Keywords:
Cyanometalates
Crystal structures
Magnetic properties
Single-molecule magnets
Polynuclear complexes

ABSTRACT

Treatment of $[NEt_4][(Tp^{*Me})Fe^{III}(CN)_3]\cdot H_2O$ with nickel(II) trifluoromethanesulfonate affords $\{[(Tp^{*Me})Fe^{III}(CN)_3]_2[Ni^{II}(DMF)_4]_2[OTf]_2\}\cdot 2DMF$ (**1**) while $\{[(Tp^{*Me})Fe^{III}(CN)_3]_2[Ni^{II}(bpy)_2]_2[ClO_4]_2\}\cdot 3MeCN\cdot 2H_2O\cdot MeOH$ (**2**) is obtained from $Ni(ClO_4)_2\cdot 6H_2O$ and 2,2′-bipyridine mixtures. In the frame of an isotropic Heisenberg model, the experimental χT versus T data were modeled well with the following best set of parameters: $J/k_B = +9.0(4)$ and $+8.5(4)$ K and $g_{av} = 2.4(1)$ and $2.5(1)$ for **1** and **2**, respectively; the first excited state ($S = 2$) for **1** and **2** are ca. 18 and 16.8 K above the $S_T = 3$ ground state. Analysis of the ac susceptibility suggests that **1** exhibits fast quantum tunneling of the magnetization above ca. 1.8 K while **2** displays slow relaxation in the range seen for many SMMs; at $H_{dc} = 2.2$ kOe an SMM energy barrier of $\Delta_{eff} = 15.7$ K is estimated for **2**. Upon prolonged standing in air, **1** is readily transformed into a new system that exhibits a respectable energy barrier ($\Delta_{eff} = 20.4$ K) suggesting that the desolvation is able to dramatically alter the dynamics and the quantum properties of the square-shaped $\{Fe^{III}_2(\mu\text{-}CN)_4Ni^{II}_2\}$SMM.

1. Introduction

Cyanometalates are an increasingly popular class of building blocks that find use in the preparation of materials, which exhibit a diverse assortment of properties such as radioactive cesium mitigation [1], room temperature magnetism [2], charge storage [3], electrochomism [4], gas separation and storage [5], and photomagnetic bistability [6,7]. Among these well-known materials are those of the three-dimensional defect solids known collectively as Prussian blues. These defect coordination networks are generally prepared using a building block synthetic approach [7] via treatment of $[M^n(CN)_x]^{n-x}$ ($x = 6$, 7, or 8) anions with a range of cationic metal ions and/or coordinatively unsaturated complexes $[M'(L)_y]^{m+}$. The ions self-assemble into a regular array of cyanido-bridged metal M(μ-CN)M′ linkages, which in the presence of charge balancing alkali metal cations (A^+) and water, produce products of a generalized $A_nM(OH_2)_{6-6m}[M'(CN)_6]_m\cdot(2-n)H_2O$ formulation.

Using the concept of dimensional reduction [8], where capping ligands are used to limit the numbers of formed M(μ-CN)M′ pairs during self-assembly, several low-dimensional systems such as single-molecule magnets (SMMs) [9–26,27a], single-chain magnets (SCMs) [27–33], and materials that exhibit dramatic changes in their magnetic and/or optical behavior [34–42] have been reported. These compounds are constructed from deliberate combination of $[(L)_yM(CN)_x]^{n-}$ salts with those containing substitutionally labile ligands to afford a predetermined number and geometric arrangement of M(μ-CN)M′ linkages [9–42], that allows for a number of precursors containing various capping ligands to self-assemble towards a common structural archetype. Assuming that formed M(μ-CN)M′ pairs are fundamentally limited by the numbers of available coordination sites and terminal cyanides present, product connectivity and stoichiometry may be predicted and controlled at the single-ion level. This strategy allows for the systematic construction of a series of structurally related polynuclear materials with tailored magnetic and optical properties [9–42].

The most common building-blocks are those of $[(Tp^R)Fe^{III}_{LS}(CN)_3]^-$ stoichiometry, where Tp^R is C_{3v}-symmetric, tridentate, and facially coordinate poly(pyrazolyl)borate ligand. These complexes find use in the construction of many SMMs owing to a favorable introduction of magnetic anisotropy via first-order orbital contributions, that appear to be collinear with their C_3 (B···Fe) rotation axes [14–26,31]. We previously reported that tuning of ancillary ligand steric demand affords a systematic means to direct self-assembly of various tricyanido $[(Tp^R)Fe^{III}(CN)_3]^-$ building blocks towards a variety of single-molecule magnet (SMMs)

* Corresponding authors. Tel.: +1 314 516 4382; fax: +1 314 516 5342 (S.M. Holmes), tel.: +33 5 56 84 56 50; fax: +33 5 56 84 56 00 (R. Clérac).
E-mail addresses: clerac@crpp-bordeaux.cnrs.fr (R. Clérac), holmesst@umsl.edu (S.M. Holmes).

0277-5387/$ - see front matter © 2012 Elsevier Ltd. All rights reserved.
http://dx.doi.org/10.1016/j.poly.2012.10.039

structural archetypes [14–26,31]. In these solids, the polypyrazolylborate (Tp^R) ligands enable coordination geometry preferences and electronic properties of derived complexes to be selectively tuned at upwards of 10 substitutable positions; this approach allows for the isolation of several tri-, tetra-, hexa-, and octanuclear complexes and one-dimensional chains that exhibit properties ranging from single-molecule magnet [9–26], photoresponsive [35–41], or single-chain magnet behavior [28–33].

As part of a continuing effort to explore new structural building units and investigate their role in directing self-assembly processes and resulting magnetic and/or optical properties of their aggregation products, we recently turned our attention towards a new building block, $[(Tp^{*Me})Fe^{III}(CN)_3]^-$, where Tp^{*Me} = tris(3,4,5-trimethylpyrazol-1-yl)borate. In comparison to Tp^* analogs [Tp^* = tris(3,5-dimethylpyrazol-1-yl)borate] addition of a single methyl group per pyrazolate unit affords a ligand that induces significant steric interactions with ancillary ligands residing on adjacent cyanido-bridged metal centers, while simultaneously enhancing solubility of the polynuclear complex [19,20]. These secondary interactions have enabled the construction of several SMMs that appear to favorably orient their angular momentum projections such that enhanced barriers to magnetization reversal are realized, in comparison to those containing comparatively smaller ligands. For example, owing to the steric demand of the Tp^{*Me} ligands present, a linear octanuclear $\{Fe^{III}_4Ni^{II}_4\}$ SMM was found to have a nearly parallel arrangement of anisotropy tensors and exhibits a high spin reversal energy barrier (Δ_{eff} = 33 K), in comparison to molecular boxes, which have rather small SMM energy barriers [19]. In the present contribution we report on two new and structurally related cyanido-bridged $\{Fe^{III}_2Ni^{II}_2\}$ square complexes: $\{[(Tp^{*Me})Fe^{III}(CN)_3]_2[Ni^{II}(DMF)_4]_2[OTf]\}_2{\cdot}2DMF$ (**1**; OTf = trifluoromethanesulfonate, DMF = dimethylformamide) and $\{[(Tp^{*Me})Fe^{III}(CN)_3]_2[Ni^{II}(bpy)_2]_2[ClO_4]_2\}{\cdot}3MeCN{\cdot}2H_2O{\cdot}MeOH$ (**2**). Their structures and magnetic properties are discussed in the frame of other pyrazolylborate-based tetranuclear analogs.

2. Experimental

2.1. General considerations

Nickel(II) trifluoromethanesulfonate, $[Ni(OTf)_2]$ [43], and $[NEt_4][(Tp^{*Me})Fe^{III}(CN)_3]{\cdot}H_2O$ [19] were prepared by literature methods. 2,2′-bipyridine (bpy, Aldrich) and $Ni(ClO_4)_2{\cdot}6H_2O$ (Acros) were used as received. The IR spectra were recorded as Nujol mulls between KBr plates on a Thermo-Electron Nicolet Impact 6700 FTIR instrument in the 400–4000 cm^{-1} region. Magnetic measurements on microcrystalline samples of **1** and **2** were obtained on Quantum Design MPMS-XL and PPMS-9 magnetometers. Alternating current (ac) susceptibility measurements were conducted using an oscillating ac field of 1 Oe with frequencies ranging from 10 to 10000 Hz. The magnetic data were corrected for the sample holder while diamagnetic contributions were estimated using Pascal's constants [44]. Elemental analyses were performed by Robertson Microlit Laboratories.

Caution! Although no problems were encountered during our studies, cyanides are toxic and perchlorate salts are potentially explosive. These should be handled with great care.

2.2. Preparation of complexes

2.2.1. $\{[(Tp^{*Me})Fe^{III}(CN)_3Ni^{II}(DMF)_4][OTf]\}_2{\cdot}2DMF$ (**1**)

Treatment of $[NEt_4][(Tp^{*Me})Fe(CN)_3]{\cdot}H_2O$ (0.122 g, 0.196 mmol) with $Ni(OTf)_2$ (0.107 g, 0.300 mmol) in DMF (10 mL) under an argon atmosphere afforded a red solution that allowed to stir for 1 h. The filtrate was layered with Et_2O (50 ml) and allowed to stand for 7 days. The dark red blocks were isolated via filtration and dried under vacuum for 2 min at room temperature. Yield: 0.116 g (56%). *Anal.* Calc.: C, 42.47; H, 6.07; N, 18.74. Found: C, 42.39; H, 5.78; N, 18.60%. IR (Nujol, cm^{-1}): 2549 (m), 2166 (s), 2118 (m), 1674 (vs), 1645 (vs), 1559 (w), 1516 (w), 1495 (m), 1457 (vs), 1377 (vs), 1271 (s), 1240 (s), 1224 (m), 1172 (w), 1145 (s), 1103 (s), 1059 (m), 1031 (s), 888 (s), 872 (m), 832 (s), 752 (w), 736 (m), 720 (m), 680 (s), 658 (w), 638 (s), 569 (w), 547 (m), 517 (m).

2.2.2. $\{[(Tp^{*Me})Fe^{III}(CN)_3]_2[Ni^{II}(bpy)_2]_2[ClO_4]_2\}{\cdot}3MeCN{\cdot}2H_2O{\cdot}MeOH$ (**2**)

Treatment of $Ni(ClO_4)_2{\cdot}6H_2O$ (0.073 g, 0.20 mmol) with bpy (0.063 g, 0.41 mmol) in MeCN (5 mL) afforded a purple mixture which was stirred for 10 min. Addition of $[NEt_4][(Tp^{*Me})Fe^{III}(CN)_3]{\cdot}H_2O$ (0.124 g, 0.200 mmol) in methanol (10 mL) afforded a dark red solution, that was filtered, and allowed to stand for 7 days. Dark red rectangular crystals were collected via filtration and dried under vacuum for 2 min at room temperature. Yield: 0.135 g (64.9%). *Anal.* Calc.: C, 51.43; H, 5.09; N, 19.54. Found: C, 50.91; H, 5.01; N, 18.99%. IR (Nujol, cm^{-1}): 3426 (br, m), 3112 (w), 3092 (w), 3079 (w), 2555 (m), 2261 (m), 2250 (m), 2155 (vs), 2129 (m), 1644 (m), 1599 (vs), 1575 (m), 1567 (s), 1520 (s), 1490 (m), 1474 (w), 1429 (s), 1386 (m), 1360 (m), 1311 (m), 1239 (vs), 1191 (w), 1172 (m), 1154 (w), 1092 (vs), 1081 (vs), 1023 (s), 1012 (m, sh), 932 (w), 921 (w), 905 (w), 887 (w), 871 (m), 833 (m), 815 (w), 771 (vs), 738 (s), 688 (m), 667 (w), 652 (m), 623 (s), 544 (w).

2.3. Structure determinations and refinements

X-ray structural data were collected at 90.0(2) and 100.0(2) K for **1** and **2**, respectively, on Nonius Kappa CCD and Bruker APEX-II CCD diffractometers. Crystals were mounted in Paratone-N oil on glass fibers and the structures were solved by direct methods (SHELXS97) [45,46] and completed by difference Fourier methods (SHELXL97) [46]. Refinement was performed against F^2 by weighted full-matrix least-squares (SHELXL97) [46], and empirical absorption corrections (SADABS) [47] were applied. Hydrogen atoms were found in difference maps and subsequently placed at calculated positions using suitable riding models with isotropic displacement parameters derived from their carrier atoms. Non-hydrogen atoms were refined with anisotropic displacement parameters and atomic scattering factors were taken from the *International Tables for Crystallography*, *vol. C* [48]. Crystal data and selected details of structure determinations and geometrical parameters appear in Tables 1 and 2.

3. Results and discussion

3.1. Synthesis and spectroscopic characterization

Treatment of a 1:1 ratio of $[NEt_4][(Tp^{*Me})Fe(CN)_3]{\cdot}H_2O$ and $Ni(OTf)_2$ in dimethylformamide affords a mixture which contains a tetranuclear complex (**1**) and $\{[(Tp^{*Me})Fe^{III}(CN)_3]_4[Ni^{II}(DMF)_3]_2\}{\cdot}4DMF{\cdot}H_2O$ [20] as the major and minor products, respectively; in the presence of a slight stoichiometric excess of $Ni(OTf)_2$ complex **1** is the sole crystalline product. The infrared spectrum of **1** exhibits medium intensity $\bar{\nu}_{BH}$ (2549 cm^{-1}) and $\bar{\nu}_{CN}$ (2118 cm^{-1}) stretches in addition to a more intense one (2166 cm^{-1}), that is higher in energy than those seen for $[NEt_4][(Tp^{*Me})Fe^{III}(CN)_3]{\cdot}H_2O$ (2119 and 2115 cm^{-1}). In **1**, we tentatively assign these $\bar{\nu}_{CN}$ stretches as bridging and terminal cyanides, respectively [20]. A second structurally related analog of **1** may also be obtained via combination of a 1:1:2 ratio of $[NEt_4][(Tp^{*Me})Fe(CN)_3]{\cdot}H_2O$, $Ni(ClO_4)_2{\cdot}6H_2O$ and 2,2′-bipyridine in acetonitrile/methanol mixtures. The infrared spectrum of the bipridine-substituted complex,

Table 1
Crystallographic data for **1** and **2**.[a–c]

Parameters	1	2
Formula	$C_{74}H_{126}B_2F_6Fe_2Ni_2N_{28}O_{16}S_2$	$C_{89}H_{105}N_{29}B_2Fe_2Ni_2Cl_2O_{11}$
Formula weight	2092.80	2078.66
λ (Å)	0.71073	0.71073
T (K)	90.0(2)	100.0(2)
Crystal system	triclinic	triclinic
Space group	$P\bar{1}$	$P\bar{1}$
a (Å)	12.5955(1)	13.431(3)
b (Å)	13.7243(1)	13.598(3)
c (Å)	14.8144(2)	15.274(3)
α (°)	85.9963(5)	82.158(6)
β (°)	75.5953(5)	68.230(5)
γ (°)	87.4564(5)	71.554(6)
V (Å^3)	2473.36(4)	2456.9(8)
Z	1	1
ρ_{calc} (mg m^{-3})	1.405	1.405
μ (mm^{-1})	0.789	0.794
R_1[b]	0.0372	0.0480
wR_2[c]	0.0897	0.1185

[a] $I \geqslant 2\sigma(I)$.
[b] $R_1 = \sum||F_o| - |F_c||/\sum|F_o|$.
[c] $wR_2 = \{\sum[w(F_o^2 - F_c^2)^2]/\sum[w(F_o^2)^2]\}^{1/2}$.

Table 2
Selected bond distances (Å) and angles (°) for **1** and **2**.

1		2	
Fe1–C1	1.926(2)	Fe1–C1	1.923(3)
Fe1–C2	1.927(2)	Fe1–C2	1.928(3)
Fe1–C3	1.930(2)	Fe1–C3	1.931(3)
Fe1–N5	1.979(2)	Fe1–N5	2.018(2)
Fe1–N7	1.995(2)	Fe1–N7	1.984(2)
Fe1–N9	2.011(2)	Fe1–N9	1.992(2)
Ni1–N1	2.026(2)	Ni1–N1	2.056(2)
Ni1–N2A	2.038(2)	Ni1–N2A	2.056(2)
Ni1–O4	2.082(2)	Ni1–N10	2.096(2)
Ni1–O5	2.050(2)	Ni1–N11	2.077(2)
Ni1–O6	2.062(2)	Ni1–N12	2.098(2)
Ni1–O7	2.123(4)	Ni1–N13	2.087(2)
C1–N1	1.147(3)	C1–N1	1.141(3)
C2–N2	1.150(3)	C2–N2	1.152(3)
C1–Fe1–C2	93.43(9)	C1–Fe1–C2	86.6(1)
C1–Fe1–C3	84.24(9)	C1–Fe1–C3	85.0(1)
C2–Fe1–C3	86.38(9)	C2–Fe1–C3	89.0(1)
Fe1–C1–N1	176.3(2)	Fe1–C1–N1	176.7(2)
Fe1–C2–N2	175.4(2)	Fe1–C2–N2	178.1(2)
Fe1–C3–N3	176.2(2)	Fe1–C3–N3	177.5(2)
N5–Fe1–N7	88.98(7)	N5–Fe1–N7	89.34(9)
N5–Fe1–N9	89.53(7)	N5–Fe1–N9	91.05(9)
N7–Fe1–N9	91.01(8)	N7–Fe1–N9	86.09(9)
N2A–Ni1–N1	89.51(7)	N1–Ni1–N2A	93.35(9)
N1–Ni1–O4	89.87(7)	N1–Ni1–N10	92.15(9)
N1–Ni1–O5	94.77(8)	N1–Ni1–N11	90.83(9)
N1–Ni1–O6	91.42(7)	N1–Ni1–N12	170.65(8)
N1–Ni1–O7	172.1(2)	N1–Ni1–N13	92.69(9)

{[(Tp^{*Me})Fe^{III}(CN)$_3$]$_2$[Ni^{II}(bpy)$_2$]$_2$[ClO$_4$]$_2$}·3MeCN·2H$_2$O·MeOH (**2**), exhibits intense $\bar{\nu}_{BH}$ and $\bar{\nu}_{CN}$ stretching absorptions ($\bar{\nu}_{BH}$ = 2545 cm^{-1}; $\bar{\nu}_{CN}$ = 2155 and 2129 cm^{-1}) that are significantly shifted in energy relative to those seen for **1** and [NEt$_4$][(Tp^{*Me})-Fe^{III}(CN)$_3$]·H$_2$O, suggesting that the electronic environments of the cyanides are quite different; additional high energy $\bar{\nu}_{CN}$ (2261 and 2250 cm^{-1}) stretches signal the presence of acetonitrile. Thermogravimetric analyses (TGA) of crystalline samples of **1** and **2** (Figs. S1 and S2) suggest that lattice solvent loss easily occurs near ca. 110 °C for **1** and at room temperature for **2** and at higher temperatures (ca. 125 and 260° C) both **1** and **2** apparently undergo decomposition.

3.2. Crystallographic studies

Compounds **1** and **2** crystallize as structurally related squares in the triclinic $P\bar{1}$ space group (Table 1). Their structures consist of centrosymmetric cyano-bridged Fe^{III}(CN)(μ-CN)$_2$Ni^{II} units with terminal cyanides adopting an anti orientation relative to the nearly planar core. In Fig. 1, the Ni^{II} ions in **1** display a distorted *cis*-Ni(NC)$_2$O$_4$ coordination environment and average Ni–N and Ni–O distances of 2.032(2) and 2.067(2) Å, respectively, are found. In **2**, the Ni^{II} ion adopts NiN$_6$ coordination consisting of two *cis*-cyano and four bidentate 2,2′-bipyridine (bpy) ligands. The average Ni–N$_{CN}$ bond in **2** [2.056(2) Å] is slightly longer than those in **1** and typical Ni–N$_{bpy}$ distances [2.090(2) Å] are found for each complex (Table 2).

In **1** and **2** the tricyanoferrate(III) anions adopt an idealized C_{3v}-symmetry that is composed of three *fac*-cyanides and a facially coordinate and tridentate Tp^{*Me} ligand. The average Fe–C [1.928(2) and 1.927(3) Å] and Fe–N [1.995(2) and 1.998(2) Å] distances are nearly identical in **1** and **2**, respectively (Table 2). In each complex the [(Tp^{*Me})Fe(CN)$_3$]$^-$ anions are linked to two adjacent [Ni(L)$_n$]$^{2+}$ units via *cis*-cyanides to form Fe^{III}(μ-CN)$_2$Ni^{II} linkages where the {Fe$_2$(μ-CN)$_4$Ni$_2$} cores have Fe···Ni contacts of 5.09 × 5.11 Å (for **1**) and 5.11 × 5.13 Å (for **2**). The Fe–C≡N–Ni linkages are nearly linear and the Fe–C–N and Ni–N–C angles are 175.8(2)° and 173.4(2)° and 177.4(2)° and 173.9(2)°, for **1** and **2**, respectively. The cationic cores of **1** and **2** are well-isolated and intercomplex Ni···Ni contacts of 8.827(2) and 9.01(2) Å are seen.

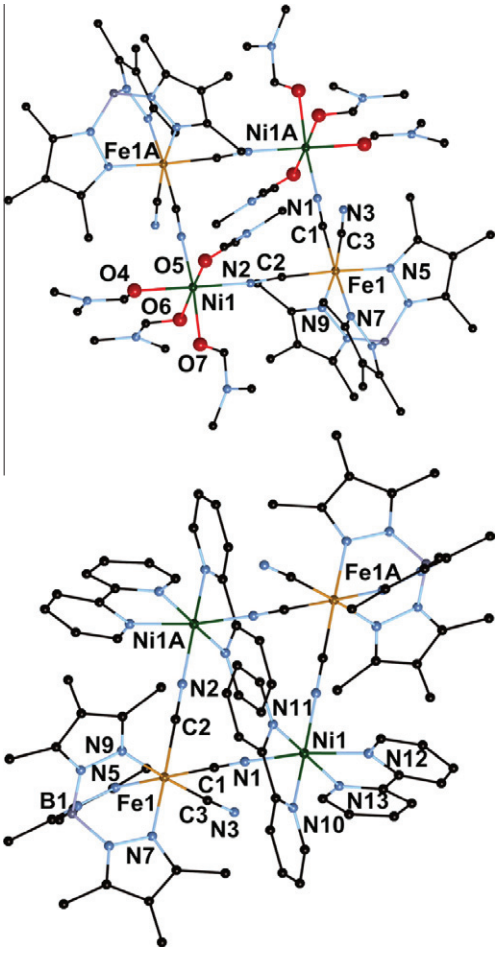

Fig. 1. X-ray structures of cationic portions of **1** (top) and **2** (bottom). All anions, lattice solvent, and hydrogen atoms are eliminated for clarity.

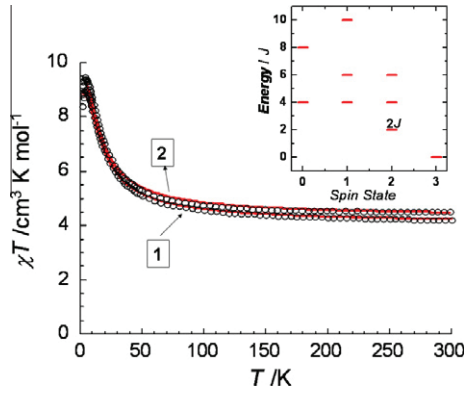

Fig. 2. Temperature dependences of the χT product (where χ is the molar magnetic susceptibility that is equal to M/H per complex) collected in an applied dc field of 1000 Oe for **1** and **2**. Inset: General energy level diagram for **1** and **2**.

The closest intercomplex contacts [3.537(3) Å] are found between the Tp^{*Me} 5-methyl group and DMF nitrogen atoms in **1**, while Ni···NC_{term} (N3···Ni1) contacts are more distant at ca. 7.569(1) Å; in **2** close contacts are present between bpy ligands [ca. 3.360(2) Å] while the Ni···NC_{term} contacts (N3···Ni) are slightly longer [7.883(7) Å] (Table 2).

3.3. Magnetic studies

3.3.1. Static magnetic properties of *1* and *2*

The temperature dependences of the χT product of **1** and **2** were collected in a static dc field of 1 kOe over a range of temperatures (1.8–300 K, Figs. 2 and S3). The χT values at room temperature [4.3 and 4.5 $cm^3\ mol^{-1}\ K$, for **1** and **2**] are in agreement with the presence of magnetically isolated Fe^{III}_{LS} ($S = ½$, $g = 2.6–2.8$) and Ni^{II} ($S = 1$, $g = 2.2–2.3$) ions in a 2:2 ratio, assuming that significant orbital contributions are present on the Fe^{III}_{LS} ions [13–20]. With decreasing temperatures, the χT values for **1** and **2** gradually increase between 300 and ca. 50 K suggesting that ferromagnetic interactions are operative; at lower temperatures maximum values of 9.1 and 9.4 $cm^3\ K\ mol^{-1}$ at 4.3 K are seen, which decreases slightly to 8.3 and 8.8 $cm^3\ K\ mol^{-1}$ at 1.8 K, for **1** and **2**, respectively.

Considering an idealized symmetrical square structure for **1** and **2**, the magnetic data were initially modeled in the frame of an isotropic Heisenberg spin Hamiltonian:

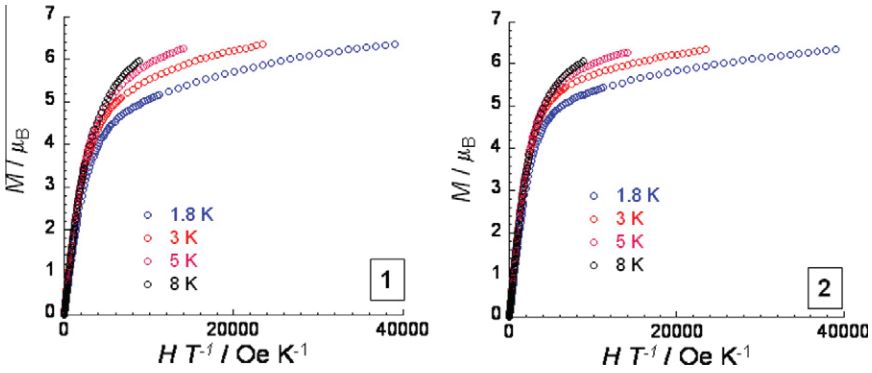

Fig. 3. M vs H/T data for **1** (left) and **2** (right) between 1.8 and 8 K with sweep-rates of 100–200 Oe/min.

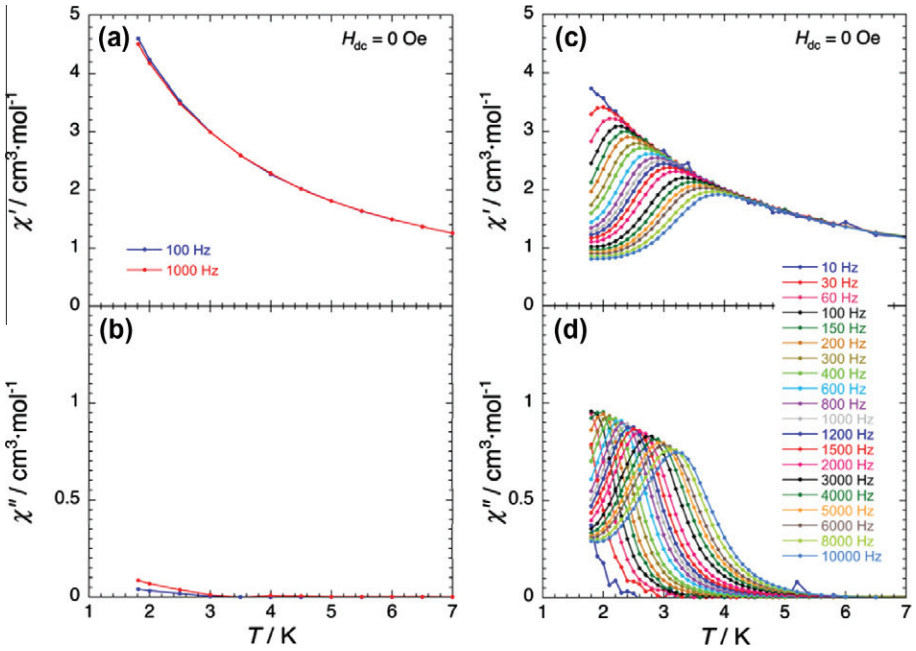

Fig. 4. Temperature dependence of the real (χ') and imaginary (χ'') components of the ac susceptibility at different frequencies between 10 and 10000 Hz on an air-dried sample of **1** measured (a and b) immediately after filtration and (c and d) after a few days in air [$H_{dc} = 0$ Oe; $H_{ac} = 1$ Oe].

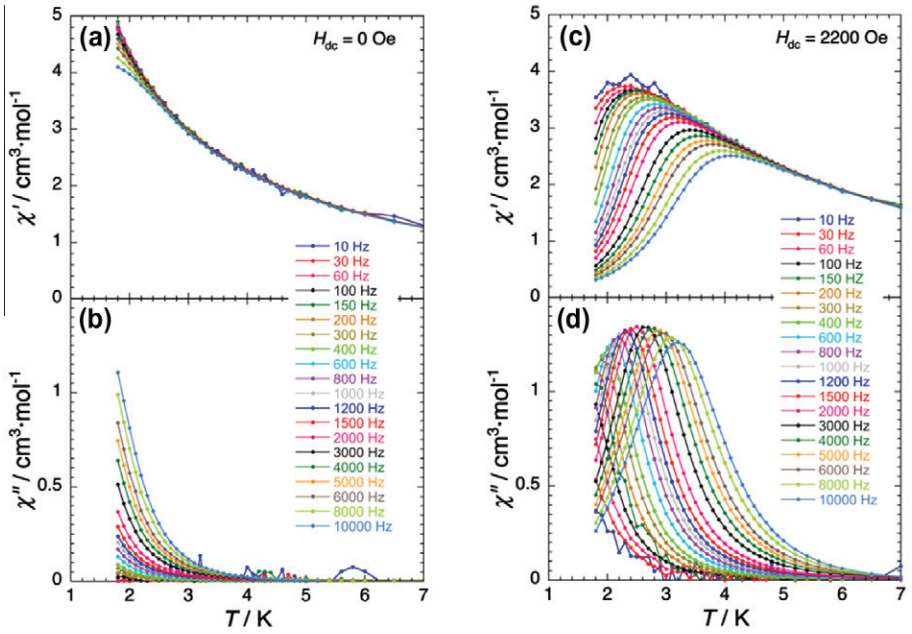

Fig. 5. Temperature dependence of the real (χ') and imaginary (χ'') components of the ac susceptibility at different frequencies between 10 and 10000 Hz [H_{ac} = 1 Oe] on an air-dried sample of **2** measured immediately after filtration at (a and b) zero applied *dc* field (H_{dc} = 0) and (c and d) at H_{dc} = 2200 Oe.

$$H = -2J((S_{Ni} + S_{NiA}) \cdot (S_{Fe} + S_{FeA})) \quad (1)$$

where J is the average exchange interaction between Fe^{III}_{LS} and Ni^{II} sites through the cyano bridge, and S_i are the spin operators for each metal ions ($S_{Ni(II)}$ = 1 and $S_{Fe(III)}$ = $^1/_2$). Subsequent application of the van Vleck equation to Kambe's vector coupling scheme allowed for an analytical expression (Eq. (2), below) of the magnetic susceptibility in the low field approximation [49]:

$$\chi = \frac{2g_{av}^2\mu_B^2}{k_BT}\left\{\frac{14\exp(10J/k_BT) + 5\exp(7J/k_BT) + 7\exp(6J/k_BT) + 6\exp(4J/k_BT) + 1}{7\exp(10J/k_BT) + 5\exp(8J/k_BT) + 12\exp(6J/k_BT) + 8\exp(4J/k_BT) + \exp(2J/k_BT) + 3}\right\} \quad (2)$$

Considering only data above 5 K to avoid the effects of intermolecular interactions and/or magnetic anisotropy, the best fit parameters are J/k_B = + 9.0(4) and + 8.5(4) K, and g_{av} = 2.4(1) and 2.5(1) for **1** and **2**, respectively; we note that attempts to fit the magnetic data using different $g_{Ni(II)}$ and $g_{Fe(III)}$ terms leads to overparameterization and gives physically unrealistic values. These values are comparable to those seen in a variety of Fe^{III}/Ni^{II} complexes containing $[(Tp^R)Fe^{III}(CN)_3]^-$ anions [19,27]. The intra-complex magnetic interactions lead to an S_T = 3 spin ground state for **1** and **2**, with first excited states, S = 2, that are close in energy at 18 and 16.8 K, respectively.

The field dependence of the magnetization collected for **1** and **2** confirms that both exhibit significant magnetic anisotropy for cyanide-based SMMs (Figs. 3 and S4). At 1.8 K and an applied dc magnetic of 7 T the magnetization values seen (6.3 μ_B for both) confirm that the S_T = 3 spin ground state is present with an associated g factor that is greater than 2. This conclusion is consistent with previously described magnetic data (e.g. χT versus T data). Furthermore, the M versus H/T data obtained for **1** and **2** are non-superimposable on a master curve and confirm that significant magnetic anisotropy is present below 8 K. Consequently, a crude estimation of the magnetic data was initiated using an S_T = 3 macro-spin model, taking into account a simple uniaxial magnetic anisotropy (with the Hamiltonian: $H = DS_{T,z}^2$); unfortunately the experimental data are not reproduced using this simplistic model indicating that low lying excited states are relevant even at 1.8 K. We note that no hysteresis is observed above 1.8 K in the M versus H data and is consistent with behavior reported for a variety of polynuclear cyanide-bridged complexes [9–26].

3.3.2. Dynamic magnetic properties of *1* and *2*

To probe the magnetization dynamics of **1** and **2** ac susceptibility measurements were performed at various frequencies in the absence and presence of a static dc magnetic field (Figs. 4 and 5 and S3–S6). In the absence of an applied dc field, weak frequency-dependent ac signals were seen below 1000 Hz for **1**, suggesting that slow magnetic relaxation may be operative below 1.8 K. However, upon prolonged standing in air in its dried form, crystalline samples of **1** begin to exhibit fully visible and frequency-dependent signals in both in-phase (χ') and out-of-phase (χ'') ac susceptibility data above 1.8 K (Fig. 4), suggesting that **1** is unstable and is easily transformed into another magnetic species; efforts to elucidate the structure via single crystal X-ray studies were met with failure. As judged from the ac magnetic data (Fig. 4), the energy gap for this material was estimated to be ca. 20 K (with $\tau_0 = 3.7 \times 10^{-8}$ s) and the temperature dependence of the relaxation time follows an Arrhenius law [$\tau = \tau_0\exp(\Delta_{eff}/k_BT)$] above 1.8 K (Fig. S5). This value is in the range expected for many related SMM materials [29]. As **1** appears to readily desolvate, as judged from TGA analysis, and given that the energy gap is ca. 20 K, it is likely that **1** undergoes facile transformation into another structural phase upon removal of DMF, while maintaining an intact $\{Fe^{III}_2Ni^{II}_2\}$ core (*vide infra*). We note that similar behavior has also been observed for structurally related $\{[(Tp^*)Fe^{III}(CN)_3]_2[M^{II}(DMF)_4]_2[OTf]_2\}\cdot 2DMF$ (M^{II} = Co, Ni) materials [16a]. As this is likely to be a general phenomenon, we propose that sample han-

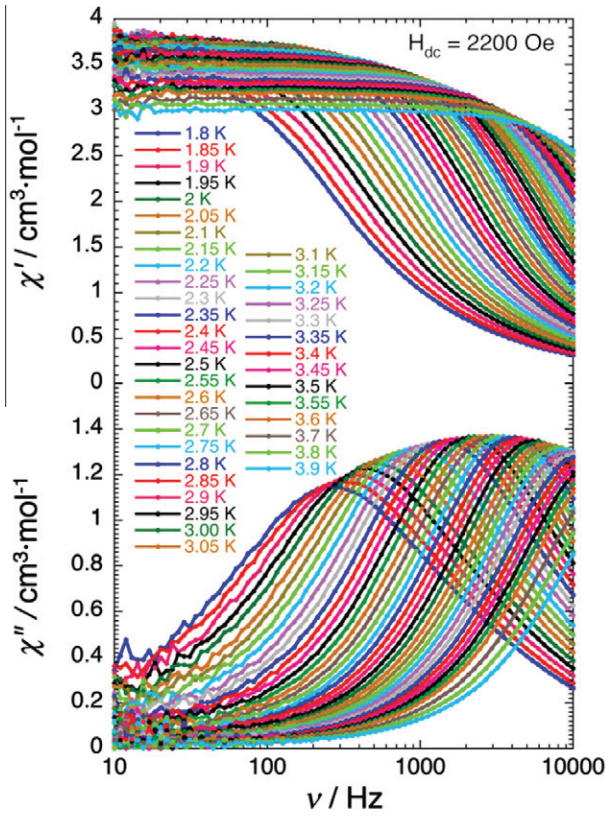

Fig. 6. Frequency dependence of the real (χ') and imaginary (χ'') components of the ac susceptibility at different temperatures between 1.8 and 3.9 K [H_{ac} = 1 Oe] on an air-dried sample of **2** measured right after filtration [H_{dc} = 2200 Oe]. The solid lines are guides for the eyes.

dling should be considered a possible route for generating ill-defined magnetic materials (e.g. desolvated), where single crystal and magnetic data are not representative of the same compound.

Rationalizing that substitution of coordinated DMF for bpy ligands should afford complexes with greater stability with regards to desolvation, and given that this qualitative trend is also seen in TGA data, a series of detailed ac susceptibility measurements were performed to ascertain whether **2** exhibits SMM behavior. Indeed, both in-phase (χ') and out-of-phase (χ'') components of the ac susceptibility at zero dc fields are frequency dependent suggesting that **2** is an SMM (Figs. 5a, b and S6). In order to further investigate its magnetization dynamics, additional ac data were collected in the presence of small dc-fields, which should act to lift the degeneracy of the magnetic m_s states and decrease the probability of quantum tunneling of the magnetization (Fig. S7). As expected, an increase of the magnetic relaxation time (or decrease of the characteristic frequency) can be followed as a function of increasing applied dc field up to 2200 Oe (Figs. 5c, d, S8 and S9). At this optimum dc field (Fig. 6), the relaxation time obeys Arrhenius behavior with $\tau_o = 1.4 \times 10^{-7}$ s and an effective energy barrier of 15.7 K is found (S10 and S11). Using this result, a crude estimation of the uniaxial anisotropy term for the $S_T = 3$ ground state is $D/k_B \leqslant -1.8$ K and confirms that **2** is an SMM that exhibits fast quantum tunneling of the magnetization in zero applied field, and a slower thermally activated relaxation times at non-zero dc fields.

4. Conclusions

Two square-shaped $\{Fe^{III}_2(\mu\text{-}CN)_4Ni^{II}_2\}$ complexes containing $[(Tp^{*Me})Fe^{III}(CN)_3]^-$ anions were synthesized and characterized. Above 1.8 K, slow relaxation of the magnetization was readily seen for **2** at zero applied magnetic fields and its relaxation rates were found to slow upon application of non-zero dc fields, affording a SMM energy barrier of Δ_{eff} = 15.7 K (for H_{dc} = 2.2 kOe). Interestingly, **1** does not exhibit appreciable SMM dynamics above 1.8 K, suggesting that fast quantum tunneling of the magnetization is operative. Nevertheless over a period of time in air, **1** slowly transforms into another species that exhibits magnetic behavior that is reminiscent of several structurally related $\{Fe^{III}_2(\mu\text{-}CN)_4Ni^{II}_2\}$ square SMM analogs (Δ_{eff} = 20.4 K).

Acknowledgments

S.M.H. gratefully acknowledges the National Science Foundation (CHE 0914935, CAREER; CHE 0939987, X-ray upgrade) and University of Missouri-St. Louis (College of Arts and Sciences Research Award) for financial support. R.C. acknowledges the University of Bordeaux, the ANR (NT09_469563, AC-MAGnets Project), the Région Aquitaine, the GIS Advanced Materials in Aquitaine (COMET Project), and the CNRS (PICS N° 4659) for financial support.

Appendix A. Supplementary material

CCDC 873805 and 873806 contains the supplementary crystallographic data for compounds **1** and **2**, respectively. These data can be obtained free of charge via http://www.ccdc.cam.ac.uk/conts/retrieving.html, or from the Cambridge Crystallographic Data Centre, 12 Union Road, Cambridge CB2 1EZ, UK; fax: (+44) 1223-336-033; or e-mail: deposit@ccdc.cam.ac.uk. Supplementary data associated with this article can be found, in the online version, at http://dx.doi.org/10.1016/j.poly.2012.10.039.

References

[1] (a) M. Shatruk, C. Avendano, K.R. Dunbar, Prog. Inorg. Chem. 56 (2009) 155. and references cited therein;
(b) K.R. Dunbar, R.A. Heintz, Prog. Inorg. Chem. 45 (1997) 283. and references cited therein.
[2] (a) S. Ferlay, T. Mallah, R. Ouahès, P. Veillet, M. Verdaguer, Nature 378 (1995) 701;
(b) S.M. Holmes, G.S. Girolami, J. Am. Chem. Soc. 121 (1999) 5593;
(c) Ø. Hatlevik, W.E. Buschmann, J. Zhang, J.L. Manson, J.S. Miller, Adv. Mater. 11 (1999) 914;
(d) R. Garde, F. Villain, M. Verdaguer, J. Am. Chem. Soc. 124 (2002) 10531.
[3] (a) C.D. Wessells, R.A. Huggins, Y. Cui, Nat. Commun. (2011), http://dx.doi.org/10.1038/ncomms1563;
(b) C.D. Wessells, S.V. Peddada, M.T. McDowell, R.A. Huggins, Y. Cui, J. Electrochem. Soc. 159 (2012) A98;
(c) C.D. Wessells, S.V. Peddada, R.A. Huggins, Y. Cui, Nano Lett. 11 (2011) 5421.
[4] (a) O. Sato, T. Iyoda, A. Fujishima, K. Hashimoto, Science 271 (1996) 49;
(b) S.-I. Ohkoshi, O. Sato, T. Iyoda, A. Fujishima, K. Hashimoto, J. Am. Chem. Soc. 120 (1998) 5349;
(c) T. Mahfoud, G. Molnar, S. Bonhommeau, S. Cobo, L. Salmon, P. Demont, H. Tokoro, S.-I. Ohkoshi, K. Boukheddaden, A. Bousseksou, J. Am. Chem. Soc. 131 (2009) 15049;
(d) M.B. Robin, Inorg. Chem. 1 (1962) 337;
(e) M.B. Robin, P. Day, Adv. Inorg. Nucl. Radiochem. 10 (1967) 247;
(f) V. Balzani, A. Juris, M. Venturi, S. Campagna, S. Serroni, Chem. Rev. 96 (1996) 759. and references cited therein;
(g) S.-I. Ohkoshi, H. Tokoro, T. Matsuda, H. Takahashi, H. Ire, K. Hashimoto, Angew. Chem., Int. Ed. Engl. 46 (2007) 3238;
(h) O. Sato, T. Iyoda, A. Fujishima, K. Hashimoto, Science 272 (1996) 704.
[5] (a) R.J. Taylor, R.S. Drago, J.E. George, J. Am. Chem. Soc. 111 (1989) 6610;
(b) S. Imamura, J.H. Lundsford, Languir 1 (1985) 326;
(c) R.J. Taylor, R.S. Drago, J.P. Hage, Inorg. Chem. 31 (1992) 253;
(d) D. Ramprasad, G.P. Pez, B.H. Toby, T.J. Markley, R.M. Pearlstein, J. Am. Chem. Soc. 117 (1995) 10694;
(e) S.S. Kaye, J.R. Long, J. Am. Chem. Soc. 127 (2005) 6506;
(f) S.S. Kaye, J.R. Long, Chem. Commun. (2007) 4486;
(g) J.T. Culp, M.R. Smith, E. Bittner, B. Bockrath, J. Am. Chem. Soc. 130 (2008) 12427;
(h) R.S. Despande, S.L. Sharp-Goldman, J.L. Wilson, A.B. Bocarsly, Chem. Mater. 15 (2003) 4239;

(i) J.N. Behera, D.M. D'Alessandro, N. Soheilnia, J.R. Long, Chem. Mater. 21 (2009) 1922.
[6] (a) Z.-Z. Gu, O. Sato, T. Iyoda, K. Hashimoto, A. Fujishima, Chem. Mater. 9 (1997) 1092;
(b) A. Bleuzen, C. Lomenech, V. Escax, F. Villain, F. Varret, C. Cartier dit Moulin, M. Verdaguer, J. Am. Chem. Soc. 12 (2) (2000) 6648;
(c) C. Cartier dit Moulin, F. Villain, A. Bleuzen, M. Arrio, P. Sainctavit, C. Lomenech, V. Escax, F. Baudelet, E. Dartyge, M. Verdaguer, J. Am. Chem. Soc. 122 (2000) 6653;
(d) V. Escax, A. Bleuzen, C.C.D. Moulin, F. Villain, A. Goujon, F. Varret, M. Verdaguer, J. Am. Chem. Soc. 123 (2001) 12536;
(e) G. Champion, V. Escax, C.C.D. Cartier, A. Bleuzen, F. Villain, F. Baudelet, E. Dartyge, M. Verdaguer, J. Am. Chem. Soc. 123 (2001) 12544;
(f) G. Molnar, S. Cobo, T. Mahfoud, E.J.M. Vertelman, P.J. van Konigsbruggen, P. Demont, A. Bousseksou, J. Chem. Phys. C 113 (2009) 2586;
(g) E.J.M. Vertelman, T.T.A. Lummen, A. Meetsma, M.W. Bouwkamp, G. Molnar, P.H.M. van Loosdrecht, P.J. van Konigsbruggen, Chem. Mater. 20 (2008) 1236;
(h) J.-H. Her, P.W. Stephens, C.M. Kareis, J.S. Moore, K.S. Min, J.-W. Park, G. Bali, B.S. Kennon, J.S. Miller, Inorg. Chem. 49 (2010) 1524;
(i) C. Tian, E. Kan, C. Lee, M.-W. Whangbo, Inorg. Chem. 49 (2010) 3086;
(j) O. Sato, Acc. Chem. Res. 36 (2003) 692.
[7] (a) A. Ludi, H. Gudel, Struct. Bonding (Berlin) 14 (1973) 1;
(b) J.M. Herra, A. Bachschmidt, F. Villain, A. Bleuzen, V. Marvaud, W. Wernsdorfer, M. Verdaguer, Philos. Trans. R. Soc. A 226 (2008) 127;
(c) M. Verdaguer, G.S. Girolami, Magnetoscience, Wiley, 2005.
[8] (a) S.C. Lee, R.H. Holm, Angew. Chem., Int. Ed. Engl. 29 (1990) 840. and references cited therein;
(b) J.R. Long, A.S. Williamson, R.H. Holm, Angew. Chem., Int. Ed. Engl. 34 (1995) 226;
(c) J.R. Long, L.S. McCarty, R.H. Holm, J. Am. Chem. Soc. 118 (1996) 4603.
[9] J.J. Sokol, A.G. Hee, J.R. Long, J. Am. Chem. Soc. 124 (2002) 7656.
[10] E.J. Schelter, F. Karadas, C. Avendano, A.V. Prosvirin, W. Wernsdorfer, K.R. Dunbar, J. Am. Chem. Soc. 129 (2007) 8139.
[11] J. Xiang, W.-L. Man, J.-F. Guo, S.-M. Yiu, G.-H. Lee, S.-M. Peng, G. Xu, S. Gao, T.-C. Lau, Chem. Commun. 46 (2010) 6102.
[12] R. Lescouëzec, L.M. Toma, J. Vaissermann, M. Verdaguer, F.S. Delgado, C. Ruiz-Pérez, F. Lloret, M. Julve, Coord. Chem. Rev. 249 (2005) 2691. and references cited therein.
[13] Y.-Z. Zhang, S. Gao, H.-L. Sun, G. Su, Z.M. Wang, S.W. Zhang, Chem. Commun. 40 (2004) 1906.
[14] D.-F. Li, R. Clérac, S. Parkin, G.-B. Wang, G.T. Yee, S.M. Holmes, Inorg. Chem. 45 (2006) 5251.
[15] Y.-Z. Zhang, U.P. Mallik, N.P. Rath, R. Clérac, S.M. Holmes, Inorg. Chem. 50 (2011) 10537.
[16] (a) D.-F. Li, S. Parkin, G.-B. Wang, G.T. Yee, A.V. Prosvirin, S.M. Holmes, Inorg. Chem. 44 (2005) 4903;
(b) D.-F. Li, R. Clérac, G.-B. Wang, G.T. Yee, S.M. Holmes, Eur. J. Inorg. Chem. (2007) 1341.
[17] K. Park, S.M. Holmes, Phys. Rev. B 74 (2006) 224440.
[18] (a) D.-F. Li, S. Parkin, G.-B. Wang, G.T. Yee, R. Clérac, W. Wernsdorfer, S.M. Holmes, J. Am. Chem. Soc. 128 (2006) 4214;
(b) D.-F. Li, S. Parkin, R. Clérac, S.M. Holmes, Inorg. Chem. 45 (2006) 7569.
[19] Y.-Z. Zhang, U.P. Mallik, N.P. Rath, G.T. Yee, R. Clérac, S.M. Holmes, Chem. Commun. 46 (2010) 4953.
[20] Y.-Z. Zhang, U.P. Mallik, R. Clérac, N.P. Rath, S.M. Holmes, Chem. Commun. 47 (2011) 7194.
[21] (a) W. Liu, C.-F. Wang, Y.-Z. Li, J.-L. Zuo, X.-Z. You, Inorg. Chem. 45 (2006) 10058;
(b) C.-F. Wang, W. Liu, Y. Song, X.-H. Zhou, J.-L. Zuo, X.-Z. You, Eur. J. Inorg. Chem. (2008) 717.
[22] D.-Y. Wu, Y.J. Zhang, W. Huang, O. Sato, Dalton Trans. 39 (2010) 5500.
[23] S. Wang, J.-L. Zuo, H.-C. Zhou, H.-J. Choi, Y. Ke, J.R. Long, X.-Z. You, Angew. Chem., Int. Ed. 43 (2004) 5940.
[24] C.-F. Wang, J.-L. Zuo, B.M. Bartlett, Y. Song, J.R. Long, X.-Z. You, J. Am. Chem. Soc. 128 (2006) 7162.
[25] S. Wang, J.-L. Zuo, H.-C. Zhou, Y. Song, S. Gao, X.-Z. You, Eur. J. Inorg. Chem. (2004) 3681.
[26] Z.-G. Gu, Q.-F. Yang, X.-H. Zhou, J.-L. Zuo, X.-Z. You, Inorg. Chem. 46 (2007) 3236.
[27] (a) L.M. Toma, R. Lescouëzec, J. Pasán, C. Ruiz-Pérez, J. Vaissermann, J. Cano, R. Carrasco, W. Wernsdorfer, F. Lloret, M. Julve, J. Am. Chem. Soc. 128 (2006) 4842.
[28] D.-P. Zhang, L.-F. Zhang, Y.-T. Chen, H.-L. Wang, Z.-H. Ni, W. Wernsdorfer, J.-Z. Jiang, Chem. Commun. 46 (2010) 3550.
[29] (a) M. Ferbinteanu, H. Miyasaka, W. Wernsdorfer, K. Nakata, K. Sugiura, M. Yamashita, C. Coulon, R. Clérac, J. Am. Chem. Soc. 127 (2005) 3090;
(b) T.D. Harris, M.V. Bennett, R. Clérac, J.R. Long, J. Am. Chem. Soc. 132 (2010) 3980;
X. Feng, T.D. Harris, J.R. Long, Chem. Sci. 2 (2011) 1688;
T. Senapati, C. Pichon, R. Ababei, C. Mathonière, R. Clérac, Inorg. Chem. 51 (2012) 3796;
(c) H. Miyasaka, T. Madanbashi, A. Saitoh, N. Motokawa, R. Ishikawa, M. Yamashita, S. Bahr, W. Wernsforfer, R. Clérac, Chem. Eur. J. 18 (2012) 3942.
[30] K. Mitsumoto, E. Oshiro, H. Nishikawa, T. Shiga, Y. Yamamura, K. Saito, H. Oshio, Chem. Eur. J. 17 (2011) 9612.
[31] S. Wang, X.-H. Ding, J.-L. Zuo, X.-Z. You, W. Huang, Coord. Chem. Rev. 255 (2011) 1713. and references cited therein.
[32] (a) S. Wang, J.-L. Zuo, S. Gao, Y. Song, H.-C. Zhou, Y.-Z. Zhang, X.-Z. You, J. Am. Chem. Soc. 126 (2004) 8900;
(b) H.-R. Wen, C.-F. Wang, Y. Song, S. Gao, J.-L. Zuo, X.-Z. You, Inorg. Chem. 45 (2006) 8942;
(c) C.-F. Wang, D.-P. Li, X. Chen, X.-M. Li, Y.-Z. Li, J.-L. Zuo, X.-Z. You, Chem. Commun. 45 (2009) 6940.
[33] (a) K. Mitsumoto, M. Ui, M. Nihei, H. Nishikawa, H. Oshio, CrystEngComm 12 (2010) 2697;
(b) N. Hoshino, Y. Sekine, M. Nihei, H. Oshio, Chem. Commun. 46 (2010) 6117.
[34] (a) M. Nihei, M. Ui, M. Yokota, L.-Q. Han, A. Maeda, H. Kishida, H. Okamoto, H. Oshio, Angew. Chem., Int. Ed. 44 (2005) 6484;
(b) M. Shatruk, A. Dragulescu-Andrasi, K.E. Chambers, S.A. Stoian, E.L. Bominaar, C. Achim, K.R. Dunbar, J. Am. Chem. Soc. 129 (2007) 6104;
(c) R. Herchel, R. Boca, M. Gembicky, J. Kozísek, F. Renz, Inorg. Chem. 43 (2004) 4103;
(d) I. Boldog, F.J. Munoz-Lara, A.B. Gaspar, M.C. Munoz, M. Seredyuk, J.A. Real, Inorg. Chem. 48 (2009) 3710.
[35] D.-F. Li, R. Clérac, O. Roubeau, E. Harté, C. Mathonière, R. Le Bris, S.M. Holmes, J. Am. Chem. Soc. 130 (2008) 252.
[36] Y.-Z. Zhang, D.-F. Li, R. Clérac, M. Kalisz, C. Mathonière, S.M. Holmes, Angew. Chem., Int. Ed. 49 (2010) 3752.
[37] D. Siretanu, D.-F. Li, L. Buisson, D.M. Bassani, S.M. Holmes, C. Mathonière, R. Clérac, Chem. Eur. J. 17 (2011) 11704.
[38] (a) M. Nihei, Y. Sekine, N. Suganami, K. Nakazawa, A. Nakao, H. Nakao, Y. Murakami, H. Oshio, J. Am. Chem. Soc. 133 (2011) 3592;
(b) C.P. Berlinguette, A. Dragulescu-Andrasi, A. Sieber, J.R. Galán-Mascarós, H.-U. Güdel, C. Achim, K.R. Dunbar, J. Am. Chem. Soc. 126 (2004) 6222;
(c) C.P. Berlinguette, A. Dragulescu-Andrasi, A. Sieber, H.-U. Güdel, C. Achim, K.R. Dunbar, J. Am. Chem. Soc. 127 (2005) 6766.
[39] T. Liu, D.-P. Dong, S. Kanegawa, S. Kang, O. Sato, Y. Shiota, K. Yoshizawa, S. Hayami, S. Wu, C. He, C.-Y. Duan, Angew. Chem., Int. Ed. 51 (2012), http://dx.doi.org/10.1002/anie.201201305.
[40] T. Liu, Y. Zhang, S. Kanegawa, O. Sato, Angew. Chem., Int. Ed. 49 (2010) 8645.
[41] T. Liu, Y.-J. Zhang, S. Kanegawa, O. Sato, J. Am. Chem. Soc. 132 (2010) 8250.
[42] J. Mercurol, Y.-L. Li, E. Pardo, O. Risset, M. Seuleiman, H. Rousselière, R. Lescouëzec, M. Julve, Chem. Commun. 46 (2010) 8995.
[43] S.M. Holmes, Molecule-Based Magnets Constructed from Hexacyanometalates, Thesis, 1999.
[44] E.A. Boudreaux, L.N. Mulay, Theory and Applications of Molecular Paramagnetism, Wiley, 1976.
[45] Z. Otwinowski, W. Minor, Methods Enzymol. 276 (1997) 307.
[46] G.M. Sheldrick, SHELX-97. Programs for Crystal Structure Solution and Refinement, University of Gottingen, Germany, 1997.
[47] G.M. Sheldrick, SADABS, An Empirical Absorption Correction Program, Bruker Analytical X-Ray Systems, Madison, WI, 1996.
[48] International Tables for Crystallography, vol. C, Kluwer Academic Publishers, Dordrecht, Netherlands, 1992.
[49] K. Kambe, J. Phys. Soc. Jpn. 5 (1950) 48.